XV International Conference on Computational Plasticity. Fundamentals and Applications
COMPLAS 2019
E. Oñate, D.R.J. Owen, D. Peric, M. Chiumenti & Eduardo de Souza Neto (Eds)

MULTISCALE MODELLING OF LIVER PERFUSION

Eduard Rohan[1], **Jana Turjanicová**[1] **and Vladimír Lukeš**[1]

[1] Faculty of Applied Sciences, European Centre of Excellence, NTIS – New Technologies for Information Society, University of West Bohemia, Univerzitní 8, 306 14 Plzeň, Czech Republic, rohan@kme.zcu.cz

Key words: Homogenization, Double Porosity, Liver Tissue, Perfusion, Darcy-Brinkman model

Abstract. We compare two homogenized models of the microcirculation which rely on different assumptions. The first model has been derived by the homogenization of the mesoscopic structure with the double-porosity medium represented by the Biot model with large contrasts in the permeability coefficients constituting the Darcy law. The newly developed so-called Biot-Darcy-Brinkman (BDB) model is described in the paper; it arises from a two-stage homogenization of the fluid-structure interaction problem which requires geometric representations of the sinusoidal and the inter-lobular vasculatures associated with venous compartments, the portal and the hepatic veins. An illustrative example shows a good correspondence between the two models.

1 Introduction

Understanding of liver perfusion on the multiple scales is crucial for the surgical treatment (liver resections, transplantations), but also for understanding how the liver perfusion is modified by diffuse parenchyma diseases such as cirrhosis, steatohepatitis, or the sinusoidal obstruction syndrome. At the macroscopic scale the liver receive blood from the two separated vascular system (trees), one belonging to the hepatic artery and other to the portal vein. These two vascular trees branch repeatedly, until they reach the microcirculation at the level of so-called hepatic units, typically considered as hexagonal lobules separated by thin vascular septum. The lobular structure can be approximated as a "locally" periodic array of honeycomb-like cells constituted by the sinusoidal porosity connecting the vertex and central veins which are the terminal branches of the two trees.

Here we focus on the lobular level perfusion whereby flows in vascular trees of the upper hierarchies can be described by the multi-compartment Darcy flow model [10]. Existing studies of the liver microcirculation [4, 3], i.e. perfusion between the portal track and the central vein at lobular level, usually consider the conception of the regular hexagonal liver lobule as the hepatic functional unit, see e.g. [5]. In [6], a convenient model has been derived by the homogenization of the mesoscopic structure with the double-porosity medium represented by the Biot model with large contrasts in the permeability coefficients

constituting the Darcy law. Within this model, the macroscopic variables represent two pressures associated with the portal and hepatic veins, representing the vertex and central blood vessels, respectively, and the two related interconnecting networks the macroscopic variables.

As the new contribution, in this paper we extend the so-called Biot-Darcy-Brinkman (BDB) model to describe structures wirth two mesoscopic system of separated channels which correspond to the lobular structure arrangement. For only one mesoscopic compartment, the model was derived using a two-level homogenization approach in [11] for rigid porous structures and then extended in [12] to deal with deformable solid phase, *i.e.* deformable hepatic cells.

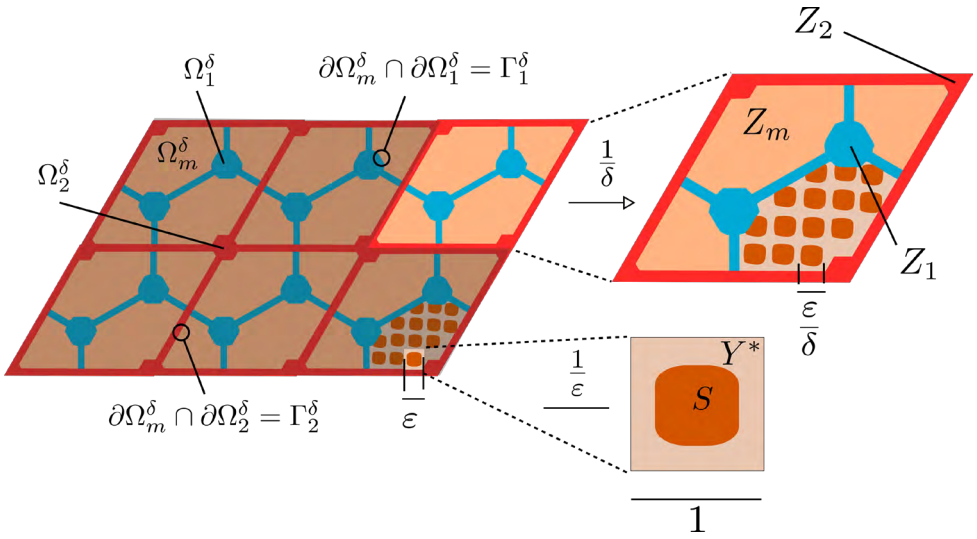

Figure 1: Lobular porous structure parameterized by ε, the characteristic size of the sinusoidal porosity, and δ which describes the size of the mesoscopic heterogeneities.

2 Biot-Darcy-Brinkman model

Two-level homogenization of the fluid-structure interaction with a scaling ansatz related to the viscosity has been applied to treat the geometry with two mesoscopic channels. The macroscopic model is defined in terms of the pressure field associated with flow in the liver sinusoids, the two velocity fields associated with the precapillary vessels of the portal and hepatic vein systems and the displacements.

2.1 Microscopic and mesoscopic structure

The liver tissue can be described using a two-level structured porous material consisting of the solid and fluid phases. These phases occupy an open bounded domain $\Omega \subset \mathbb{R}^3$ which can be decomposed in dual way. According to the phases, Ω splits into the fluid Ω_f and solid Ω_s parts separated by the solid interface $\Gamma_{\rm fs} = \overline{\Omega_f} \cap \overline{\Omega_s}$, whereby both Ω_s and Ω_f are connected domains. The hierarchical structure is periodic at the micro- and meso-scopic

scales related to two small parameters ε and δ, respectively, see Fig. 1. At the mesoscopic scale, the periodic structure is formed by two families of fluid filled channels occupying domains Ω_α^δ, $\alpha = 1, 2$, whereby $\Omega_c^\delta = \bigcup_\alpha \Omega_\alpha^\delta$, and by domain $\Omega_m^\delta = \Omega \setminus \Omega_c^\delta$ which is constituted by a microporous material representing the so-called sinusoidal porosity. In addition, domain $\Omega_p^{\varepsilon,\delta} \subset \Omega_m^\delta$ represents micro pores saturated by fluid, whereas $\Omega_s^{\varepsilon,\delta} = \Omega_m^\delta \setminus \Omega_p^{\varepsilon,\delta}$ is the skeleton. To summarize the decompositions,

$$\begin{aligned} \Omega &= \Omega_m^\delta \cup \Omega_c^\delta \cup \Gamma^\delta \ , \\ \text{solid (hepatic cells)} \quad & \Omega_s^{\varepsilon,\delta} \subset \Omega_m^\delta \ , \\ \text{microporosity (sinusoids)} \quad & \Omega_p^{\varepsilon,\delta} = \Omega_m^\delta \setminus \Omega_s^{\varepsilon,\delta} \ , \\ \text{fluid (blood)} \quad & \Omega_f = \Omega_p^{\varepsilon,\delta} \cup \Omega_c^\delta \cup \Gamma_{cp}^{\varepsilon,\delta} \ . \end{aligned} \tag{1}$$

The mesoscopic channels Ω_α^δ, $\alpha = 1, 2$, are mutually disconnected by the sinusoidal porosity Ω_m^δ, so that also two disconnected interfaces are defined, $\Gamma_\alpha^\delta = \partial\Omega_\alpha^\delta \cap \partial\Omega_m^\delta$.

The sinusoidal porosity (microporous material) Ω_m is generated as a periodic lattice by repeating the representative volume element (RVE) occupying domain $Y^\varepsilon = \varepsilon Y$. The zoomed cell $Y = \Pi_{i=1}^3]0, \bar{y}_i[\subset \mathbb{R}^3$ splits into the solid part (hepatic tissue) occupying domain Y_s and the complementary fluid part Y_fn (the sinusoids), see Fig. 1(a), thus $Y = Y_s \cup Y_f \cup \Gamma_Y$, where $Y_s = Y \setminus Y_f$ and $\Gamma_Y = \overline{Y_s} \cap \overline{Y_f}$ represents the sinusoidal walls on which the chemical transport and diffusion processes take place.

At the mesoscopic level, the lobular structure is generated by the periodic cell δZ representing the lobular unit, see Fig. 1(b). The zoomed cell Z involved in the homogenized model consists of microporous part situated in $Z_m \subset Z$ and of the fluid channels $Z_c = Z \setminus Z_m$, *i.e.* $Z_m \cap Z_c = \emptyset$. According to the split of Ω_c^δ, the two compartments Ω_α^δ are generated by the representative sub-cells Z_α, $\alpha = 1, 2$, whereby two interfaces $\Gamma_\alpha^Z = \overline{Z_m} \cap \overline{Z_\alpha}$ generate Γ_α^δ for a given scale δ.

By virtue of the two-level homogenization, when passing to the limit $\varepsilon \to 0$, the sinusoidal porosity is upscaled, thus yielding the mesoscopic model of the lobular structure. Consequently, pursuing $\delta \to 0$ yields the macroscopic model.

2.2 Microscopic model

At the microscopic level, we consider the fluid-structure interaction problem for a viscous incompressible fluid and elastic solid with linear material response and linear strains; for the displacement field $\boldsymbol{u}(x,t)$ with $x \in \Omega_s^{\varepsilon,\delta}$ and time $t \geq 0$, the strain components are $e_{ij}(\boldsymbol{u}) = 1/2(\partial_j u_i + \partial_i u_j)$. The elasticity tensor $\mathbb{D} = (D_{ijkl})$ satisfies the usual symmetries. saturating the micro- and the mesoscopic pores, see (1). Following the works [2], cf. [11], dealing with models of the rigid double porous media, the viscosity $\eta^{\varepsilon,\delta}$ is given by piece-wise constant function according the micropore size ε:

$$\eta^{\varepsilon,\delta} = \begin{cases} \varepsilon^2 \bar{\eta}_p & \text{in} \quad \Omega_p^{\varepsilon,\delta} \ , \\ \eta_c & \text{in} \quad \Omega_c^\delta \ . \end{cases} \tag{2}$$

This scaling of the viscosity in micropores (sinusoids) is the standard consequence of the assumed non-slip boundary condition for the flow velocity on the pore wall, cf. [1].

The problem imposed in Ω at the microlevel is constituted by the following equations and boundary and interface conditions governing the displacement $\boldsymbol{u}$ of the solid and both the fluid pressure and velocity fields $(\boldsymbol{v}^f, p)$:

$$\begin{aligned} -\nabla\cdot\mathbb{D}\boldsymbol{e}(\boldsymbol{u}) &= \boldsymbol{f}^s \quad \text{in } \Omega_s\ , \\ \boldsymbol{n}\cdot\mathbb{D}\boldsymbol{e}(\boldsymbol{u}) &= \boldsymbol{n}\cdot\boldsymbol{\sigma}^f \quad \text{on } \Gamma_{\rm fs}\ , \\ \boldsymbol{n}\cdot\mathbb{D}\boldsymbol{e}(\boldsymbol{u}) &= \boldsymbol{g}^s \quad \text{on } \partial_\sigma\Omega_s\ , \\ \boldsymbol{u} &= \boldsymbol{0} \quad \text{on } \partial_u\Omega_s\ , \end{aligned} \tag{3}$$

$$\begin{aligned} -\nabla\cdot(2\eta\boldsymbol{e}(\boldsymbol{v}^f) - p\boldsymbol{I}) &= \boldsymbol{f}^f \quad \text{in } \Omega_f\ , \\ \nabla\cdot\boldsymbol{v}^f &= 0 \quad \text{in } \Omega_f\ , \\ \boldsymbol{v}^f &= \dot{\boldsymbol{u}} \quad \text{on } \Gamma_{\rm fs}\ , \\ \boldsymbol{v}^f - \dot{\tilde{\boldsymbol{u}}} =: \boldsymbol{w} &= \bar{\boldsymbol{w}} \quad \text{on } \partial_v\Omega_f\ , \end{aligned} \tag{4}$$

where $\boldsymbol{\sigma}^f = \varepsilon^2\bar{\eta}_p\boldsymbol{e}(\boldsymbol{v}^f) - p\boldsymbol{I}$ is the fluid stress, $\boldsymbol{f}^{s,f}$ denotes the volume forces in the solid, or in the fluid, and $\boldsymbol{g}^s$ is the surface traction stresses acting on the solid part.

Above, to introduce the relative fluid velocity $\boldsymbol{w} = \boldsymbol{v}^f - \dot{\tilde{\boldsymbol{u}}}$ in the fluid-saturated pores $\Omega_f^{\varepsilon\delta}$, we define a smooth extension $\tilde{\boldsymbol{u}}$ of the displacement field $\boldsymbol{u}$ from Ω_s to entire Ω, such that $\tilde{\boldsymbol{u}} \equiv \boldsymbol{u}$ in Ω_s.

2.3 Mesoscopic model relevant to the lobular structure

The mesoscopic model obtained by the first level asymptotic analysis of (3)-(4) with the viscosity (2) for $\varepsilon \to 0$, whereas δ being fixed, is constituted by the following equations,

$$\begin{aligned} -\nabla\cdot(\mathbb{A}\boldsymbol{e}(\boldsymbol{u}^\delta) - \boldsymbol{B}p_m^\delta) &= \phi_s\boldsymbol{f}^s + \phi_f\boldsymbol{f}^f\ , \\ \boldsymbol{B}:\boldsymbol{e}(\dot{\boldsymbol{u}}^\delta) - \nabla\cdot\boldsymbol{K}(\nabla p_m^\delta - \boldsymbol{f}^f) &= 0\ , \quad \text{in } \Omega_m^\delta\ , \\ -\eta_c\nabla^2(\boldsymbol{w}^{\alpha,\delta} + \dot{\tilde{\boldsymbol{u}}}^\delta) + \nabla p_\alpha^\delta &= \boldsymbol{f}^f\ , \quad \text{in } \Omega_\beta^\delta\ , \quad \beta = 1,2\ , \\ \nabla\cdot(\boldsymbol{w}^{\alpha,\delta} + \dot{\tilde{\boldsymbol{u}}}^\delta) &= 0\ , \quad \text{in } \Omega_\beta\ , \\ \boldsymbol{n}^{[\beta]}\cdot\boldsymbol{\sigma}^{m,\delta} - p_m^\delta\boldsymbol{n}^{[\beta]} &= 0\ , \ \text{on } \Gamma_\beta\ , \\ \boldsymbol{n}^{[\beta]}\cdot(\boldsymbol{w}^{m,\delta} - \boldsymbol{w}^{\beta,\delta}) &= 0\ , \quad \text{on } \Gamma\ , \\ \boldsymbol{n}^{[\beta]}\cdot(2\eta_c\boldsymbol{e}(\boldsymbol{w}^{\alpha,\delta} + \dot{\tilde{\boldsymbol{u}}}^\delta) - p_\alpha^\delta\boldsymbol{I}) &= -p_m^\delta\boldsymbol{n}^{[\beta]}\ , \quad \text{on } \Gamma_\beta\ , \end{aligned} \tag{5}$$

where $\boldsymbol{w}^{m,\delta} = -\boldsymbol{K}(\nabla p_m^\delta - \boldsymbol{f}^f)$ is the mesoscopic flow in the sinusoidal microporosity and $\boldsymbol{\sigma}^{m,\delta} := \mathbb{A}\boldsymbol{e}(\boldsymbol{u}^\delta) - \boldsymbol{B}p_m^\delta$ is the total stress in the microporosity. It is worth to note that the interface conditions are obtained as the byproduct of the 1st level homogenization step without any restriction on the curvature of Γ_β.

2.4 Macroscopic model — BDB model for two mesoscopic channels

The macroscopic model is derived using the asymptotic analysis of (5) for $\delta \to 0$. When compared to the model of a mesoscopic structure containing only one channel system treated in [12], *i.e.* when $\alpha = 1$, thus $\Omega_1^\delta = \Omega_c^\delta$, the upscaled mesoscopic structures involving two mesoscopic channels yield two macroscopic velocity fields $\boldsymbol{w}^{0,\alpha}$, $\alpha = 1, 2$ which describe the two parallel flows associated with the portal vein and the hepatic vein compartments.

The local mesoscopic characteristic problems are defined in terms of bilinear forms:

$$\begin{aligned} a_m(\boldsymbol{u},\, \boldsymbol{v}) &= \fint_{Z_m} \mathbb{A}\boldsymbol{e}_z(\boldsymbol{u}) : \boldsymbol{e}_z(\boldsymbol{v}) \,, \\ b_m(p,\, \boldsymbol{v}) &= \fint_{Z_m} p\boldsymbol{B} : \boldsymbol{e}_z(\boldsymbol{v}) \,, \\ c_m(p,\, q) &= \fint_{Z_m} \nabla_z q \cdot \boldsymbol{K} \nabla_z p \,. \end{aligned} \tag{6}$$

Characteristic responses in the matrix part Z_m are defined as solutions of the four uncoupled problems: Find $\boldsymbol{\omega}^{ij}, \boldsymbol{\omega}^P \in \mathbf{H}^1_\#(Z_m)/\mathbb{R}^3$, and $\pi^k, \varphi^k \in H^1_\#(Z_m)$ such that

$$\begin{aligned} a_m\left(\boldsymbol{\omega}^{ij},\, \boldsymbol{v}\right) &= -a_m\left(\boldsymbol{\Pi}^{ij},\, \boldsymbol{v}\right) \quad \forall \boldsymbol{v} \in \mathbf{H}^1_\#(Z_m) \,, \\ a_m\left(\boldsymbol{\omega}^{P},\, \boldsymbol{v}\right) &= b_m(1,\, \boldsymbol{v}) - \fint_{\Gamma_c} \boldsymbol{n}^{[\mathrm{m}]} \cdot \boldsymbol{v} \quad \forall \boldsymbol{v} \in \mathbf{H}^1_\#(Z_m) \,, \\ c_m\left(\pi^k,\, q\right) &= -c_m(z_k,\, q) \quad \forall q \in H^1_\#(Z_m) \,, \\ c_m\left(\varphi^k,\, q\right) &= \fint_{\Gamma_c} q n_k^{[\mathrm{c}]} \quad \forall q \in H^1_\#(Z_m) \,, \end{aligned} \tag{7}$$

where $\Gamma_c = \Gamma_1 \cup \Gamma_2$ employed in $(7)_{2,4}$ includes both the interfaces and $\boldsymbol{\Pi}^{ij} = (\Pi_k^{ij})$ with $\Pi_k^{ij} = z_j \delta_{ik}$ is also employed below.

In each of the mesoscopic channels Z_α, the following problem must be solved. Find $(\boldsymbol{\psi}^{\alpha,ij}, \hat{\varphi}^{\alpha,ij}) \in \mathbf{H}^1_\#(Z_\alpha)/\mathbb{R}^3 \times L^2(Z_\alpha)$, such that,

$$\begin{aligned} 2\eta_c \int_{Z_\alpha} \boldsymbol{e}_z(\boldsymbol{\psi}^{\alpha,ij}) : \boldsymbol{e}_z(\boldsymbol{\vartheta}) - \int_{Z_\alpha} \hat{\varphi}^{\alpha,ij} \nabla_z \cdot \boldsymbol{\vartheta} &= -2\eta_c \int_{Z_\alpha} \boldsymbol{e}_z(\boldsymbol{\Pi}^{ij}) : \boldsymbol{e}_z(\boldsymbol{\vartheta}) \,, \\ \int_{Z_\alpha} q \nabla_z \cdot \boldsymbol{\psi}^{\alpha,ij} &= -\int_{Z_\alpha} q \nabla_z \cdot \boldsymbol{\Pi}^{ij} \,, \end{aligned} \tag{8}$$

for all $(\boldsymbol{\vartheta}, q) \in \mathbf{H}^1_\#(Z_\alpha) \times L^2(Z_\alpha)$.

The set of HC is identified in the two-scale limit equations,

$$
\begin{aligned}
\mathcal{A}_{ijkl} &= \fint_{Z_m} \mathbb{A}\boldsymbol{e}_z(\boldsymbol{\Pi}^{kl}+\boldsymbol{\omega}^{kl}) : \boldsymbol{e}_z(\boldsymbol{\Pi}^{ij}+\boldsymbol{\omega}^{ij}) \,, \\
\mathcal{B}_{ij} &= \phi_c\delta_{ij} + b_m\left(1,\, \boldsymbol{\Pi}^{ij}+\boldsymbol{\omega}^{ij}\right) - \fint_{\Gamma_Z} \boldsymbol{n}^{[\mathrm{m}]}\cdot\boldsymbol{\omega}^{ij} \,, \\
\mathcal{K}_{ij} &= \fint_{Z_m} \nabla_z(z_j+\pi^j)\cdot\boldsymbol{K}\nabla_z(z_i+\pi^i) \,, \\
\mathcal{M} &= \fint_{Z_m} M + b_m\left(1,\, \boldsymbol{\omega}^P\right) + \fint_{\Gamma_Z} \boldsymbol{n}^{[\mathrm{c}]}\cdot\boldsymbol{\omega}^P \,, \\
\mathcal{S}^\alpha_{ijkl} &= 2\eta_c \fint_{Z_\alpha} \boldsymbol{e}_z(\boldsymbol{\Pi}^{ij}+\boldsymbol{\psi}^{ij}) : \boldsymbol{e}_z(\boldsymbol{\Pi}^{kl}+\boldsymbol{\psi}^{kl}) \,, \\
\mathcal{H}^{\alpha\beta}_{ij} &= \fint_{\Gamma_\alpha} \varphi^{j,\beta} n_i^{[\alpha]} = c_m\left(\varphi^{i,\alpha},\, \varphi^{j,\beta}\right) \,, \\
\mathcal{Q}^\alpha_{ij} &= \fint_{Z_m} \nabla_z z_i\cdot\boldsymbol{K}\nabla_z\varphi^{j,\alpha} = -\fint_{Z_m} \nabla_z\pi^i\cdot\boldsymbol{K}\nabla_z\varphi^{j,\alpha} = \fint_{\Gamma_Z} \pi^i n_j^{[\alpha]} \,.
\end{aligned}
\tag{9}
$$

The alternative expressions hold due to the characteristic problems (7) and (8). I addition, the following coefficients are employed,

$$
\begin{aligned}
\mathcal{P}^\alpha_{ij} &= \phi_\alpha\delta_{ij} - \mathcal{Q}^\alpha_{ij} \,, \\
\mathcal{R}^\alpha_{ij} &= \fint_{Z_\alpha} \hat{\varphi}^{ij,\alpha} \,, \quad \mathcal{R}^\alpha_{ij} = \mathcal{R}^\alpha_{ji} \,.
\end{aligned}
\tag{10}
$$

Then the average of the pressure in the α-mesoscopic channels $\hat{p}^\alpha$ can be expressed,

$$
P^0_\alpha(x,t) = \phi_\alpha^{-1} \fint_{Z_\alpha} \hat{p}^\alpha(x,\cdot,t) = \phi_\alpha^{-1}\boldsymbol{\mathcal{R}}^\alpha : \boldsymbol{e}(\boldsymbol{w}^{0,\alpha}+\dot{\boldsymbol{u}}^0) + p^0 \,. \tag{11}
$$

This expression reveals that the mesoscopic pressure P^0_α deviates from the micropore pressure p^0 by the $\boldsymbol{\mathcal{R}}^\alpha$-projection of the mesoscopic fluid velocity deformation.

The macroscopic model involves displacement field $\boldsymbol{u}^0$, two velocity fields $\boldsymbol{w}^{0,\alpha}$, $\alpha=1,2$ associated with the two intralobular venous systems (the portal and the hepatic veins) and the pressure p^0 related to the sinusoidal micro-porosity . The quadruple of functions $(\boldsymbol{u}^0, \boldsymbol{w}^{0,\alpha}, p^0)$ satisfy the following differential equations in domain Ω,

$$
\begin{aligned}
-\nabla\cdot\left(\boldsymbol{\mathcal{A}}\boldsymbol{e}_x(\boldsymbol{u}^0) - p^0\boldsymbol{\mathcal{B}}\right) + \sum_{\beta=1,2}\boldsymbol{h}^{0,\beta} &= \boldsymbol{f}^{\mathrm{blk}} \,, \\
\boldsymbol{\mathcal{B}} : \boldsymbol{e}_x(\dot{\boldsymbol{u}}^0) + \nabla\cdot\boldsymbol{j}^0 + \mathcal{M}\dot{p}^0 &= 0 \,, \\
-\nabla\cdot\boldsymbol{\mathcal{S}}^\alpha\boldsymbol{e}_x(\boldsymbol{w}^{0,\alpha}+\dot{\boldsymbol{u}}^0) - \boldsymbol{h}^{0,\alpha} &= 0 \,, \quad \alpha=1,2 \,,
\end{aligned}
\tag{12}
$$

where $\boldsymbol{f}^{\mathrm{blk}}$ is the bulk volume force (including the forces in the fluid and solid phases) the

fluxes $\boldsymbol{h}^{0,\alpha}$ and $\boldsymbol{j}^0$ are defined, as follows:

$$\begin{aligned} \text{rate of momentum} \quad & \boldsymbol{h}^{0,\alpha} = -(\boldsymbol{\mathcal{P}}^\alpha)^T(\nabla_x p^0 - \boldsymbol{f}^f) - \sum_{\beta=1,2} \boldsymbol{\mathcal{H}}^{\alpha\beta}\boldsymbol{w}^{0,\beta} \,, \\ \text{seepage flow in the sinusoids:} \quad & \boldsymbol{j}^0 = -\boldsymbol{\mathcal{K}}(\nabla_x p^0 - \boldsymbol{f}^f) - \sum_{\beta=1,2} \boldsymbol{\mathcal{P}}^\beta \boldsymbol{w}^{0,\beta} \,. \end{aligned} \tag{13}$$

The boundary conditions are prescribed according to the boundary partitioning of $\partial\Omega$,

$$\begin{aligned} &\partial\Omega = \partial_w^\alpha\Omega \cup \partial_p^\alpha\Omega \,, \quad \partial_w^\alpha\Omega \cap \partial_p^\alpha\Omega = \emptyset \,, \quad \alpha = 1,2 \,, \\ &\partial\Omega = \partial_w^0\Omega \cup \partial_p^0\Omega \,, \quad \partial_w^0\Omega \cap \partial_p^0\Omega = \emptyset \,, \\ &\partial\Omega = \partial_\sigma\Omega \cup \partial_u\Omega \,, \quad \partial_\sigma\Omega \cap \partial_u\Omega = \emptyset \,. \end{aligned} \tag{14}$$

The Dirichlet conditions prescribed for $\boldsymbol{u}^0$, $\boldsymbol{w}^{0,\alpha}$ and p^0 can be imposed,

$$\begin{aligned} \boldsymbol{u}^0 &= \bar{\boldsymbol{u}}^0 \quad \text{on } \partial_u\Omega \,, \\ p^0 &= \bar{p}^0 \quad \text{on } \partial_p^0\Omega \,, \\ \boldsymbol{w}^{0,\alpha} &= \bar{\boldsymbol{w}}^\alpha \quad \text{on } \partial_w^\alpha\Omega \,. \end{aligned} \tag{15}$$

The complementary Neumann-type boundary conditions can be specified through given $\boldsymbol{g}, \bar{p}^0, \bar{W}_n$,

$$\begin{aligned} \boldsymbol{n}\cdot\big(\boldsymbol{\mathcal{A}}\boldsymbol{e}_x(\boldsymbol{u}^0) - p^0\boldsymbol{\mathcal{B}}\big) = \boldsymbol{n}\cdot\boldsymbol{\sigma}^{\rm mp} &= -\bar{\phi}_c\bar{p}^0\boldsymbol{n} + \bar{\phi}_m\bar{\phi}_s\boldsymbol{g} \quad \text{on } \partial_\sigma\Omega \,, \\ \boldsymbol{n}\cdot\boldsymbol{j}^0 = \bar{W}_n^{\rm mes} &= -\bar{\phi}_m\bar{\phi}_f\bar{w}_n^{\rm mic} + \bar{\phi}_c\bar{w}_n^{\rm mes} \quad \text{on } \partial_w^0\Omega \,, \\ \boldsymbol{n}\cdot\boldsymbol{\mathcal{S}}^\alpha\boldsymbol{e}_x(\boldsymbol{w}^{0,\alpha} + \dot{\boldsymbol{u}}^0) - \bar{\phi}_\alpha P_\alpha^0\boldsymbol{n} = \boldsymbol{n}\cdot\boldsymbol{\sigma}^{f,\alpha} &= -\boldsymbol{n}\bar{\phi}_\alpha(\bar{P}^\alpha - \bar{p}^0) \quad \text{on } \partial_p^\alpha\Omega \,. \end{aligned} \tag{16}$$

To explain the meaning of the Neumann conditions, the overall traction stress is by summation of $(16)_1$ and $(16)_3$ which yields $\boldsymbol{n}\cdot(\boldsymbol{\sigma}^{\rm mp} + \sum_\alpha \boldsymbol{\sigma}^{f,\alpha}) = \bar{\phi}_m\bar{\phi}_s\boldsymbol{g} - \boldsymbol{n}\sum_\alpha \bar{\phi}_\alpha\bar{P}_\alpha^0$. The fluid outflow $\bar{W}_n^{\rm mes}$ on $\partial_w^0\Omega$ is given by $\bar{w}_n^{\rm mes} = \sum_\alpha \phi_\alpha\bar{\boldsymbol{w}}^\alpha\cdot\boldsymbol{n}$ lowered by the outflow through the micropores.

We shall now consider special boundary conditions for which the weak formulation will be presented. The microporosity is supposed to be nondrained so that $\partial_p^0\Omega = \emptyset$ and $\boldsymbol{n}\cdot\boldsymbol{j}^0 = 0$ on $\partial_w^0\Omega$. For the two mesoscopic compratments, only the Dirichlet conditions will be prescribed for $\boldsymbol{n}\cdot\boldsymbol{w}^{0,\alpha}$, *i.e.* for the normal component of the velocity on the entire surface $\partial_w^\alpha\Omega = \partial\Omega$. All these assumptions yield vanishing (or natural) Neumann conditions for the flows represented by p^0 and $\boldsymbol{w}^{0,\alpha}$. For the deformation field, the Dirichlet conditions $(15)_1$ are presscribed, whereas the surface tractions $\boldsymbol{g}$ loading the solid phase must be complemented by the microporosity pressure extrapolated by the trace of the solution, *i.e.* $\bar{p}^0 = p^0$ on $\partial_\sigma\Omega$. (Unfortunately, this extra term corrupts symmetry of the entire system.)

The Dirichet conditions are respected by the function spaces,

$$\begin{aligned} V_0(\Omega) &= \{\boldsymbol{v}\in\mathbf{H}^1(\Omega)|\ \boldsymbol{v} = \boldsymbol{0} \ \text{ on } \partial_u\Omega\} \,, \\ Q_0(\Omega) &= \{q\in H^1(\Omega)|\ \int_\Omega q = 0\} \,, \\ W_0^\alpha &= \{\boldsymbol{\psi}\in\mathbf{H}^1(\Omega)|\ \boldsymbol{\psi}\cdot\boldsymbol{n} = 0 \ \text{ on } \partial_w^\alpha\Omega\} \,. \end{aligned} \tag{17}$$

Weak formulation for the BDB model Find $(\boldsymbol{u}^0, p^0, \boldsymbol{w}^{0,1}, \boldsymbol{w}^{0,2})$ such that $\boldsymbol{u}^0 \in \bar{\boldsymbol{u}}^0 + V_0(\Omega)$, $p^0 \in Q_0$ and $\boldsymbol{w}^{0,\alpha} \in \bar{w}_n^\alpha + W_0(\Omega)$ satisfy

$$\int_\Omega \left(\boldsymbol{\mathcal{A}}\boldsymbol{e}_x(\boldsymbol{u}^0) - p^0\boldsymbol{\mathcal{B}}\right) : \boldsymbol{e}_x(\boldsymbol{v}) - \sum_\alpha \int_\Omega \boldsymbol{v}\cdot\left[(\boldsymbol{\mathcal{P}}^\alpha)^T(\nabla_x p^0 - \boldsymbol{f}^f) - \sum_{\beta=1,2}\boldsymbol{\mathcal{H}}^{\alpha\beta}\boldsymbol{w}^{0,\beta}\right] =$$
$$-\int_{\partial_\sigma\Omega}\bar{\phi}_c p^0\boldsymbol{n}\cdot\boldsymbol{v} + \int_\Omega \boldsymbol{f}^{\rm blk}\cdot\boldsymbol{v} + \int_{\partial_\sigma\Omega}\boldsymbol{v}\cdot\bar{\phi}_m\bar{\phi}_s\boldsymbol{g}\ ,$$
$$\int_\Omega q\left(\boldsymbol{\mathcal{B}} : \boldsymbol{e}_x(\dot{\boldsymbol{u}}^0) + \mathcal{M}\dot{p}^0\right) + \int_\Omega \nabla q\cdot\left(\boldsymbol{\mathcal{K}}(\nabla_x p^0 - \boldsymbol{f}^f) + \sum_{\beta=1,2}\boldsymbol{\mathcal{P}}^\beta\boldsymbol{w}^{0,\beta}\right) = 0\ ,$$
$$\int_\Omega \boldsymbol{e}_x(\boldsymbol{\psi}) : \boldsymbol{\mathcal{S}}^\alpha\boldsymbol{e}_x(\boldsymbol{w}^{0,\alpha} + \dot{\boldsymbol{u}}^0) + \int_\Omega \boldsymbol{\psi}\cdot\left[(\boldsymbol{\mathcal{P}}^\alpha)^T(\nabla_x p^0 - \boldsymbol{f}^f) - \sum_{\beta=1,2}\boldsymbol{\mathcal{H}}^{\alpha\beta}\boldsymbol{w}^{0,\beta}\right] = 0\ , \alpha = 1,2\ , \tag{18}$$

for all $\boldsymbol{v} \in V_0(\Omega)$, $q \in Q_0(\Omega)$, and $q \in W_0^\alpha(\Omega)$, $\alpha = 1, 2$.

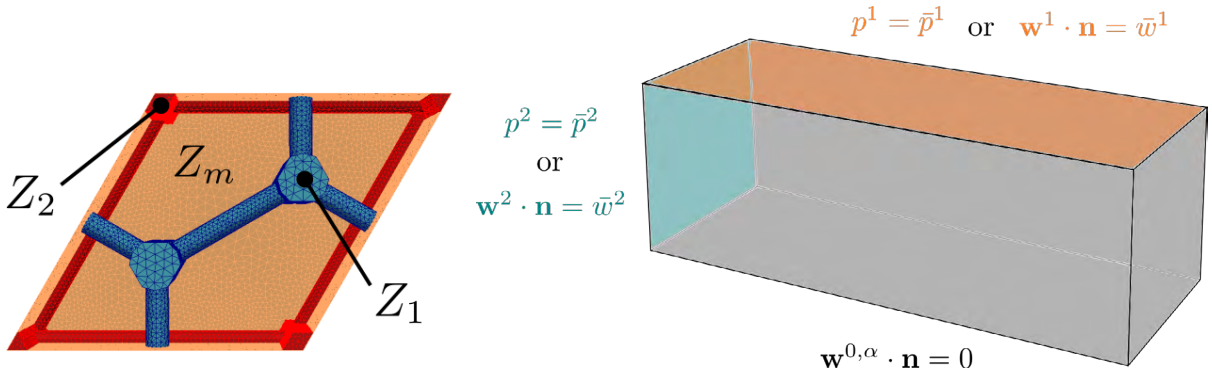

Figure 2: (a) Mesoscopic geometry representing lobular structure; (b) Macroscopic sample with boundary conditions for the two models, BDB and DD. The Dirichlet conditions defined in terms of $\bar{p}^1$ and $\bar{p}^2$ are employed for the DD model, while the normal velocities $\boldsymbol{n}\cdot\boldsymbol{w}^\alpha$, $\alpha = 1, 2$ are employed for the BDB model.

3 Numerical example and comments

In this section we compare steady state responses of the Biot-Darcy-Brinkman (BDB) model presented above with corresponding responses of the two-compartment Darcy flow model derived in [6] by the homogenization of a double-porous medium, as announced in the introduction. Below, this model is referred as the DD model. In the steady state associated with both the models, the flow and fluid pressure is decoupled from the deformation which, thus, is not discussed in this example.

The effective homogenized parameters are calculated using the representative volume element whose the structure, *i.e.* the geometry of the subdomains mimics the hepatic

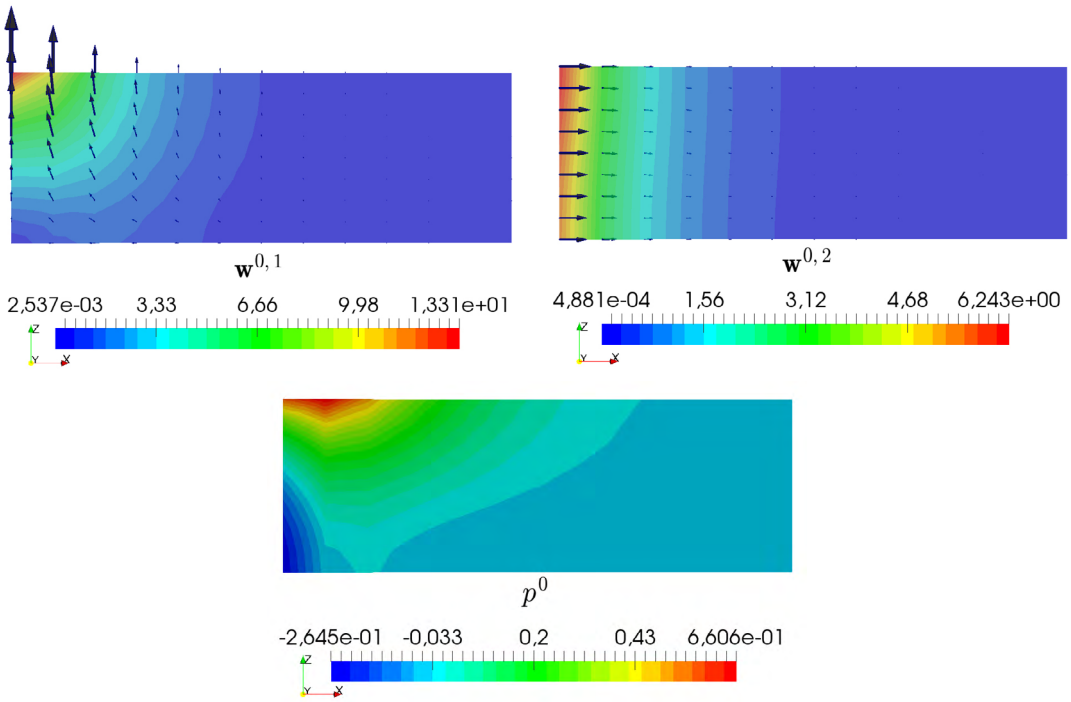

Figure 3: Macroscopic solution of BDB model. The pressure p^0 is related to the sinusoidal microporosity.

vasculature at the lobular level, see Fig. 2a. The periodic representative cell Z consists of the solid porous part Z_m reflecting the sinusoidal microporosity and two fluid parts Z_α, $\alpha = 1, 2$ representing the portal and the hepatic vascular networks in the lobules. Apart of the geometry at both the micro- and meso-scopic levels, the BDB model is defined by the fluid (blood) viscosity, while the DD model requires the permeability tensors to be defined for both the sinusoidal porosity and for the mesoscopic channels representing the precapillary vessels. To be able to compare results provided by both the models, these permeabilities are calculated from the Poiseuille law using viscosities employed in the BDB model. The macroscopic simulation is performed on a block sample, see Fig. 2b. On two distinct faces of the macroscopic sample, we prescribe the two pressures, in the case of the DD model, or normal-projected velocities, in the case of the BDB model. The other faces of the sample are assumed to be impermeable for both the models.

The macroscopic response of the BDB model, *i.e.* the solution of (18), is shown in Fig. 3. It consists of the velocity in the portal system $\boldsymbol{w}^{0,1}$, the velocity in the central system $\boldsymbol{w}^{0,2}$ and the pressure in sinusoidal microporosity p^0. In comparison, the macroscopic solution of DD model, as shown in Fig. 4) consists of the two pressure fields p^1 and p^2 referring to the pressure in the portal and central system, respectively. The velocities $\boldsymbol{w}^{0,1}_{DD}$ and $\boldsymbol{w}^{0,2}_{DD}$ in both system have to be computed from their respective pressure fields. When comparing the preliminary result of velocity $\boldsymbol{w}^{0,1}$ to velocity $\boldsymbol{w}^{0,1}_{DD}$ and velocity $\boldsymbol{w}^{0,2}$ to velocity $\boldsymbol{w}^{0,2}_{DD}$, the satisfactory qualitative and even quantitative agreement can be found. Nonsteady responses of the BDB model will be reported in a forthcoming publication.

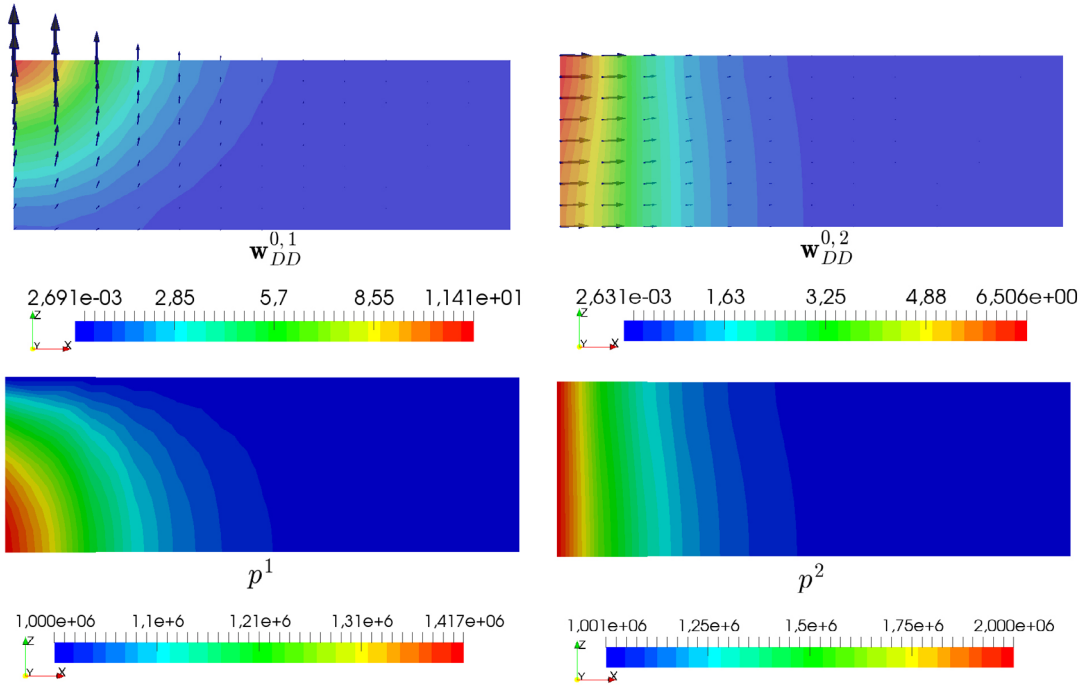

Figure 4: Macroscopic solution of DD model. Velocities $\boldsymbol{w}_{DD}^{0,\alpha}$, $\alpha = 1, 2$ in the mesoscopic porosities are directly related to the pressures p^α through the homogenized Darcy law.

Acknowledgment This research is supported by part by project GACR 19-04956S of the Scientific Foundation of the Czech Republic and by the project LO 1506 of the Czech Ministry of Education, Youth and Sports. The work was also supported from European Regional Development Fund-Project "Application of Modern Technologies in Medicine and Industry" (No. CZ.02.1.01/0.0/0.0/17_048/0007280).

REFERENCES

[1] Arbogast, T., Douglas, Jr, J. and Hornung, U. Derivation of the double porosity model of single phase flow via homogenization theory. *SIAM J. Math. Anal.* (1990) **21**(4):823–836.

[2] D. Cioranescu, A. Damlamian, G. Griso, and et al. The Stokes problem in perforated domains by the periodic unfolding method. new trends in continuum mechanics. *Theta Series in Advanced Mathematics*, **3** (2005): 67–80.

[3] Debbaut, C., Segers, P., Cornillie, P., Casteleyn, C., Dierick, M., Laleman, W. and Monbaliu, D. Analyzing the human liver vascular architecture by combining vascular corrosion casting and micro-CT scanning: a feasibility study. *J. Anat.* (2014) **224**(4):509–517.

[4] Debbaut, C., Vierendeels, J., Casteleyn, C., Cornillie, P., Van Loo, D., Simoens, P., Van Hoorebeke, L., Monbaliu, D. and Segers, P. Perfusion characteristics of the

human hepatic microcirculation based on three-dimensional reconstructions and computational fluid dynamic analysis. *J.Biomech. Eng.* (2012) **134**(1):011003.

[5] Ricken, T., Dahmen, U. and Dirsch, O. A biphasic model for sinusoidal liver perfusion remodeling after outflow obstruction. *Biomechanics and modeling in mechanobiology* (2010) **9**(4):435–450.

[6] Rohan, R. and Cimrman, R. Two-scale modeling of tissue perfusion problem using homogenization of dual porous media. *Int. J. Multiscale Comput. Eng.* (2010) **8**(1):81–102.

[7] Rohan, E., Naili, S., Cimrman, R. and Lemaire, T. Multiscale modeling of a fluid saturated medium with double porosity: Relevance to the compact bone. *J. Mech. Phys. Solids* (2012) **60**(5):857–881.

[8] E. Rohan and V. Lukesš. Modeling nonlinear phenomena in deforming fluid-saturated porous media using homogenization and sensitivity analysis concepts. Applied Mathematics and Computation, 267 (2015) 583-595.

[9] E. Rohan, V. Lukeš, J. Turjanicová, and , and R. Cimrman. Two level homogenization of flows in deforming double porosity media: Biot-Darcy-Brinkman model. In: XIV International Conference on Computational Plasticity. Fundamentals and Applications, COMPLAS XIV, E. Onate, et al. (Eds), CIMNE, Barcelona, 2017.

[10] E. Rohan, V. Lukeš, and A. Jonašová, Modeling of the contrast-enhanced perfusion test in liver based on the multi-compartment flow in porous media. In: Journal of Mathematical Biology 2 (2018), pp. 421-454.

[11] E. Rohan, J. Turjanicová, J. and V. Lukeš, A Darcy-Brinkman model of flow in double porous media – two-level homogenization and computational modelling. Computers & Structures, 207 (2018), pp. 95-110.

[12] E. Rohan, J. Turjanicová, J. and V. Lukeš, The Biot-Darcy-Brinkman model of flow in deformable double porous media; homogenization and numerical modelling. Computers and Mathematics with Applications, *In Press.* DOI:10 1016/j.camwa.2019.04.004. (2019)